

NASA TECHNICAL NOTE



NASA TN D-6419

C.1

NASA TN D-6419

LOAN COPY: RETURN  
AFWL (DOUL)  
KIRTLAND AFB, N



INELASTIC SCATTERING CALCULATIONS  
WITH PROJECTED HARTREE-FOCK WAVE  
FUNCTIONS — COUPLED CHANNEL TREATMENT

*by Robert J. Ascuitto, Richard C. Braley,  
and William F. Ford*

*Lewis Research Center  
Cleveland, Ohio 44135*



0132845

1. Report No. <b>NASA TN D-6419</b>		2. Government Accession No.		3. Recipient's Catalog No.	
4. Title and Subtitle <b>INELASTIC SCATTERING CALCULATIONS WITH PROJECTED HARTREE-FOCK WAVE FUNCTIONS - COUPLED CHANNEL TREATMENT</b>				5. Report Date <b>September 1971</b>	
				6. Performing Organization Code	
7. Author(s) <b>Robert J Ascutto, Richard C. Braley, and William F. Ford</b>				8. Performing Organization Report No. <b>E-6068</b>	
				10. Work Unit No. <b>129-02</b>	
9. Performing Organization Name and Address <b>Lewis Research Center National Aeronautics and Space Administration Cleveland, Ohio 44135</b>				11. Contract or Grant No.	
				13. Type of Report and Period Covered <b>Technical Note</b>	
12. Sponsoring Agency Name and Address <b>National Aeronautics and Space Administration Washington, D. C. 20546</b>				14. Sponsoring Agency Code	
15. Supplementary Notes					
16. Abstract  <p>For the first time a completely microscopic coupled-channel study of proton inelastic scattering is made. Proton scattering from <math>^{20}\text{Ne}</math> and from <math>^{24}\text{Mg}</math> is investigated. At least the <math>0^+</math>, <math>2^+</math>, and <math>4^+</math> members of the ground-state rotational band of each nucleus are included explicitly in the coupled equations. The nuclear wave functions are obtained by projecting states of good angular momentum from deformed Hartree-Fock intrinsic states. The scattering results are compared with the distorted wave Born approximation (DWBA) and experiment. Truncation of the nuclear model space is also investigated. The results obtained with the microscopic model confirm conclusions drawn earlier based on the macroscopic model. The shapes and deformations predicted by the macroscopic model are well reproduced by the projected Hartree-Fock model which is based purely on energy considerations.</p>					
17. Key Words (Suggested by Author(s)) <b>Hartree-Fock Coupled channels Nuclei Scattering</b>			18. Distribution Statement <b>Unclassified - unlimited</b>		
19. Security Classif. (of this report) <b>Unclassified</b>	20. Security Classif. (of this page) <b>Unclassified</b>	21. No. of Pages <b>22</b>	22. Price* <b>\$3.00</b>		

# INELASTIC SCATTERING CALCULATIONS WITH PROJECTED HARTREE-FOCK WAVE FUNCTIONS - COUPLED CHANNEL TREATMENT

by Robert J. Ascuitto,\* Richard C. Braley, and William F. Ford

Lewis Research Center

## SUMMARY

The inelastic scattering of protons by  $^{20}\text{Ne}$  and  $^{24}\text{Mg}$  is investigated using a technique (coupled channels) that explicitly includes the effect of the low-lying nuclear states. These states are represented by many-nucleon wave functions obtained by extracting the appropriate rotational component from an intrinsic Hartree-Fock wave function. The cross sections obtained in this way are compared with others obtained in the usual sort of calculation (distorted wave Born approximation), in which the effects of all nuclear states are lumped into the optical potential. The results show that, although angular distributions for the first level can be calculated correctly using the simpler method, those for the higher levels are given accurately only in the coupled channel approximation, and not always then. The variation between the two methods is different for each nucleus, and the reasons for this are discussed and shown to support the validity of the Hartree-Fock model. Finally, the lack of agreement between the experimental and theoretical cross-section magnitudes is discussed, and it is suggested that the problem is not with the nuclear wave functions, but apparently (and rather unexpectedly) with either the two-body force or the reaction mechanism.

## INTRODUCTION

In recent years, a great deal of interest has developed in understanding inelastic nucleon scattering in terms of the correlations responsible for the nuclear transition. Until very recently (ref. 1), calculations have been restricted to nuclei, which are well described by the "shell model" and "vibrational model" (refs. 2 and 3). In both descriptions, relatively simple (inert-core) nucleonic configurations are considered

---

\* Assistant Professor of Physics, Yale University, New Haven, Connecticut.

dominant components in the wave functions, thereby simplifying the calculation of form factors needed to describe the inelastic scattering.

A wealth of experimental data also exists for scattering from strongly collective nuclei, since these have the largest inelastic cross sections. Unfortunately, the enhanced transition strength in these nuclei is an indication of strongly correlated motion among many nucleons, so that a description in terms of only a few active (extracore) nucleons is likely to fail. We therefore use a microscopic picture. By this we mean that the nucleus is described in terms of the interactions between all the nucleons. Furthermore, the scattering will be described microscopically in the sense that the interaction between projectile and target shall be a sum of two-body interactions between projectile and target nucleons.

In an effort to examine how the participation of the "core nucleons" affects transition strengths, Love and Satchler introduced a core polarization model (ref. 4). This procedure essentially enhances the usual transition amplitude by addition of a term that simulates the activity of the core by means of the collective model. A more complete microscopic description of the core participation in inelastic scattering has been given by Braley and Ford (ref. 1). Core polarization effects were included explicitly by allowing all of the deformed orbitals to vary in a Hartree-Fock (HF) calculation. The wave functions obtained from that calculation were subsequently used in a distorted wave Born approximation (DWBA) study of inelastic proton scattering to the first  $2^+$  state in neon-20 ( $^{20}\text{Ne}$ ). It was found that the major effect of core polarization for the  $0_1^+ - 2_1^+$  transition was to increase the magnitude of the cross section.

In contrast to the microscopic model, the macroscopic collective model absorbs all knowledge of the underlying correlations by parameterizing this information in terms of surface deformations which can be related to various transitions of the nucleus (ref. 5).

Although this approach has been extremely successful in reproducing experimental results, it leaves one with a very limited knowledge of the nucleus and the corresponding inelastic scattering process. In the (microscopic) HF approach, collectivity or deformed shapes are explained as a consequence of the self-consistent field generated by the interacting nucleons. Naturally, this is done in some approximation that neglects certain correlations. However, it has the appealing feature that deformation parameters may be retrieved while, at the same time, the nuclear state is described in terms of the individual nucleonic motion. Of course, the validity of the HF method rests largely on comparison with experimental data. Nevertheless, one might also expect to gain some insight into the inadequacies of the microscopic model by examining the interplay between it and the macroscopic model.

Recent analysis of proton inelastic scattering on certain s-d shell nuclei, using the macroscopic model, showed evidence of strong hexadecapole shape deformation in addition to the usual quadrupole shape deformation (ref. 6). To reproduce these

moments, or the corresponding multipole transition strengths needed in the inelastic scattering, would be a strict test of the Hartree-Fock scheme. In the present calculation, we have tried to see how well we could reproduce these experimental results using the Hartree-Fock method to generate the intrinsic states  $\phi_K$ . The ground-state rotational band is obtained by projecting states of good angular momentum from the intrinsic state. The s-d shell nuclei have the advantage that the number of nucleons is sufficiently small so that HF calculations can be carried out with all particles active (i.e., no core). This allows us to study problems such as basis truncation in a convenient way since all particles are treated on an equal footing.

A coupled channel (CC) calculation of proton inelastic scattering is carried out for neon-20 ( $^{20}\text{Ne}$ ) and magnesium-24 ( $^{24}\text{Mg}$ ). In each case, at least the  $0^+$ ,  $2^+$ , and  $4^+$  members of the ground-state band were included explicitly in the coupled equations. The CC results are then compared with results of the DWBA. In an attempt to make the comparison with DWBA meaningful a special effort is made to choose DWBA optical model parameters that yield the same elastic scattering as the CC study. This procedure should remove doubts that would normally be raised because of differences in the elastic scattering that would manifest themselves in the inelastic cross sections by means of the distorted waves.

## NUCLEAR STRUCTURE INFORMATION AND CALCULATIONAL PROCEDURE

### Structure

The wave functions for the states of interest in  $^{20}\text{Ne}$  and  $^{24}\text{Mg}$  are obtained by projecting states of good angular momentum from an axially symmetric intrinsic HF state  $\phi_K$ ; that is,

$$\psi_{JM}^{(A)} = P_{MK}^J \phi_K \quad (1a)$$

where (ref. 7)

$$P_{MK}^J = \frac{2J+1}{8\pi^2} \int d\Omega D_{MK}^J(\Omega)^* R(\Omega) \quad (1b)$$

In the standard approach one generates a rotational band by projection from a single Slater determinant,  $\phi_K$

Most of the predicted nuclear properties that will be studied involve reduced matrix elements of sums of single particle operators,<sup>1</sup> that is,

$$\Omega = \sum_{n=1}^A \Omega(\vec{x}_n) \quad (4)$$

When this is the case, the reduced matrix elements may be expressed as (ref. 8)

$$\langle f || \Omega || i \rangle_{JM} = \sum_{ab} S_J(if|ab) \langle b || \Omega || a \rangle_{JM} \quad (5)$$

where a and b label single-particle states and

$$S_J(if|ab) = \sum_{J'} U(j_a J' J J_f; J_i j_b) \langle \phi_{fb}^{J'} || \phi_{ia}^{J'} \rangle \quad (6)$$

The reduced overlap integral  $\langle \phi_{fb}^{J'} || \phi_{ia}^{J'} \rangle$  involves initial and final nuclear states  $\phi_i$  and  $\phi_f$  with the single-particle states  $\phi_a$  and  $\phi_b$  projected out. When the deformed HF method with projection (ref. 7) is used to obtain the initial and final nuclear states, the reduced overlap integral may be expressed as (ref. 1)

$$\begin{aligned} \langle \phi_{fb}^{J_c} || \phi_{ia}^{J_c} \rangle &= \sum_{\lambda\lambda'} C_a^\lambda (C_b^{\lambda'})^* \sum_{MM'} \langle J_c M, j_a m | J_i K \rangle \\ &\times \langle J_c M', j_b m' | J_f K' \rangle \frac{2J_c + 1}{2} \int_0^\pi d_{M'M}^{J_c}(\theta) \Delta(\theta) \rho_{\lambda'\lambda}(\theta) \sin \theta d\theta \end{aligned}$$

where

$$\Delta(\theta) = \langle \phi_{K'} | e^{-i\theta J_y} | \phi_K \rangle$$

$$\rho_{\lambda'\lambda}(\theta) = (\tilde{B}^{-1})_{\lambda\lambda'}$$

$$B_{\lambda\lambda'}(\theta) = \langle \lambda | e^{-i\theta J_y} | \lambda' \rangle$$

---

<sup>1</sup>Expressions for the operators used in the present calculations may be found in ref. 5.

The calculation of the projected energy spectrum is more complicated since the nuclear Hamiltonian  $\mathcal{H}$  contains two-body operators in addition to the one-body kinetic energy terms. One must evaluate

$$E_J = \langle \phi_K | \mathcal{H} P_{KK}^J | \phi_K \rangle / \langle \phi_K | P_{KK}^J | \phi_K \rangle \quad (7)$$

There are several methods that may be used to carry out the energy projection (ref. 7). The most efficient of these is one in which the rotations are carried out explicitly. This technique is discussed in detail elsewhere (ref. 9).

## Scattering

Inelastic scattering based on microscopic nuclear descriptions has been considered by several authors. The coupled-channel approach to inelastic scattering has been discussed by Glendenning (ref. 2). This treatment involves the solution of a set of differential equations subject to the boundary condition that there be outgoing waves in all channels  $c$  but incoming waves only in the elastic channel  $c_0$ :

$$\left[ \frac{\hbar^2}{2m} \left( \frac{d^2}{dr^2} - \frac{l(l+1)}{r^2} \right) - U_{\text{opt}}^c(r) + E_c \right] U_{cc_0}^{\pi I}(r) = \sum_{c' \neq c} \langle \phi_{c\pi I}^{M1} | V | \phi_{c'\pi I}^{M1} \rangle U_{c'c_0}^{\pi I}(r) \quad (8)$$

where  $E_c$  is the channel energy and the functions  $\phi$  represent a vector coupling of the spin-orbit functions of relative motion ( $Y_{LSj}$ ) and the nuclear state functions ( $\psi_{JM}$ ) to a total angular momentum  $I$ . When the effective nucleon-nucleus interaction  $V$  can be expanded in irreducible tensors one finds that (ref. 2)

$$\begin{aligned} \langle \phi_{c\pi I}^M | V | \phi_{c'\pi I}^M \rangle &= (2I+1) \left[ \frac{2J_1+1}{2J_2+1} \right]^{1/2} \sum_{LSJ} (-1)^{L+S} V_S \\ &\times U(j_2 I J J_1; J_2 j_1) \langle j_2 || \mathcal{T}_{LSJ} || j_1 \rangle \langle \alpha_2 J_2 || V_{LSJ}(r, \vec{A}) || \alpha_1 J_1 \rangle \end{aligned} \quad (9)$$

where  $(\alpha_1 J_1)$  and  $(\alpha_2 J_2)$  refer to the initial and final nuclear states, respectively, and  $j_1$  and  $j_2$  to the initial and final projectile states. The reduced matrix elements of  $V_{LSJ}(r, \vec{A})$  can be obtained, when the nuclear wave functions are of the projected HF type, by the methods outlined in reference 8. Matrix elements of  $V$  diagonal in the channel index  $c$  are parameterized with the standard optical model potential (ref. 8)

$$U_{\text{opt}}(r) = V_c(r) - V_0 \rho_V(r) + 4iW_{\text{S}^2\text{S}} \frac{d}{dr} \rho_S(r) + V_{\text{LS}} \left( \frac{\hbar}{m_\pi c} \right)^2 \frac{\vec{\sigma} \cdot \vec{l}}{r} \frac{d}{dr} \rho_{\text{LS}}(r) \quad (10)$$

The nondiagonal elements are calculated with a nucleon-nucleus interaction that is a sum of potentials representing the nucleon-nucleon interaction. These two-body potentials have the simple form (ref. 1)

$$v(r) = -52 \exp \left[ -\left( \frac{r}{1.85} \right)^2 \right] (P_{\text{TE}} + 0.6 P_{\text{SE}}) \quad (11)$$

where  $P_{\text{TE}}$  and  $P_{\text{SE}}$  are projection operators for the triplet-even and singlet-even states, respectively. We recognize that even for the nondiagonal matrix elements, a renormalized interaction should be used; however, we feel that the preliminary nature of this investigation does not warrant the additional complexity. In addition we have neglected the knock-out exchange amplitudes (refs. 10 and 11) since we feel, in many instances, their importance has been overestimated.

Nuclear structure information enters the scattering calculation through structure amplitudes characterizing an elementary transition between nuclear states. These quantities are simply related to the  $S_J$ 's which were defined in equation (6) and which express the likelihood that a transition will proceed via a scattering through the configuration (a,b). The structure factors have been calculated for HF model spaces composed of six, 10, and 15 orbitals in order to study the way in which truncation of the model space affects inelastic scattering. These spaces are defined in table I.

TABLE I. - DESCRIPTION OF BASIS SPACES TO  
BE USED IN HARTREE-FOCK CALCULATIONS

Space	Basis
1	$(1s_{1/2}, 2s_{1/2}, 1d_{3/2}, 1d_{5/2}) (1p_{1/2}, 1p_{3/2})$
2	$(1s_{1/2}, 2s_{1/2}, 1d_{3/2}, 1d_{5/2})$ $(1p_{1/2}, 1p_{3/2}, 2p_{1/2}, 2p_{3/2}, 1f_{5/2}, 1f_{7/2})$
3	$(1s_{1/2}, 2s_{1/2}, 1d_{3/2}, 1d_{5/2}, 3s_{1/2}, 2d_{3/2},$ $2d_{5/2}, 1g_{7/2}, 1g_{9/2})$ $(1p_{1/2}, 1p_{3/2}, 2p_{1/2}, 2p_{3/2}, 1f_{5/2}, 1f_{7/2})$

## RESULTS WITH SIMPLE HARTREE-FOCK MODEL

The simple Hartree-Fock model has received a great deal of attention in the last few years. The prediction of many gross nuclear properties of light nuclei, based on the use of this model has been quite successful (refs. 1, 7, and 12). However, use of even the largest available model spaces in such studies seems to fall short in predicting the magnitudes of various transition rates, and intrinsic quadrupole moments. Bassichis et al (ref. 12) have found that model spaces containing as many as 21 basis states do not yield intrinsic quadrupole moments which have converged, and Ford, Braley, and Bar-Touv (ref. 13) have found similar results for projected E2 rates using model spaces containing up to 15 orbitals (refs. 12 and 13). In spite of these temporary short comings, the value of the simple HF approximation as a research tool is quite apparent and has been used to describe the nuclei of interest here ( $^{20}\text{Ne}$  and  $^{24}\text{Mg}$ ).

Wave functions for  $^{20}\text{Ne}$  and  $^{24}\text{Mg}$ , which are used to generate nuclear form factors, are obtained from reference 10. The relevant model spaces are defined in table I. A brief review of some of the structure results from reference 10 appear in tables II(a) and (b). (The projected energy spectra may be found in figs. 1 and 2.) The oscillator parameters ( $b = \sqrt{\hbar\omega/m}$ ) used in these cases were chosen to reproduce the experimental RMS radii since the two-body force used in the structure calculations was nonsaturating and the size of the basis was not sufficiently large to provide the correct long range behavior of the wave function (ref. 13). In both cases the use of a more realistic two-body force would probably result in smaller oscillator lengths to repro-

TABLE II - COMPARISON OF PREDICTED AND EXPERIMENTAL  
RADII AND E2 RATES

(a) Neon-20				
	$\langle R^2 \rangle^{1/2},$ fm	$B(E2; 0^+ - 2^+),$ $e^2 \cdot \text{fm}^4$	$B(E2; 2^+ - 4^+),$ $e^2 \cdot \text{fm}^4$	$B(E2; 4^+ - 6^+),$ $e^2 \cdot \text{fm}^4$
Predicted	2.78	204	103	90
Experiment	2.79	286±15	89±9	129±13

(b) Magnesium-24			
	$\langle R^2 \rangle^{1/2},$ fm	$B(E2; 0^+ - 2^+),$ $e^2 \cdot \text{fm}^4$	$B(E2; 2^+ - 4^+),$ $e^2 \cdot \text{fm}^4$
Predicted	3.04	374	191
Experiment	3.02±0.03	436±46	133±13

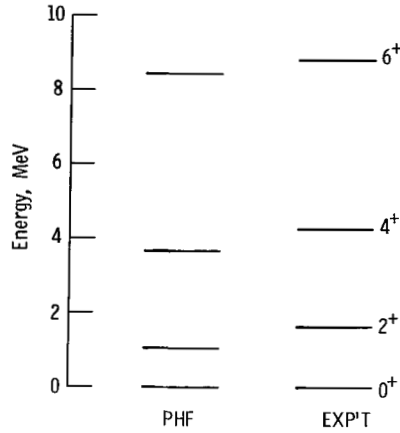


Figure 1. - Experimental and projected Hartree-Fock energy spectrum for neon-20 with  $b = 1.93$  fm.

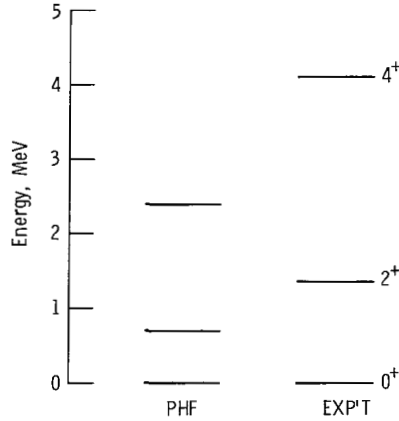


Figure 2. - Experimental and projected Hartree-Fock energy spectrum for magnesium-24 with  $b = 2.09$  fm.

duce the same radii. It is difficult to predict how this might affect the transitions rates and other properties that are known to be sensitive to the long range behavior of the wave function.

Coupled channel and DWBA calculations were carried out for 24.5-MeV proton scattering from  $^{20}\text{Ne}$ . The  $0^+$ ,  $2^+$ ,  $4^+$ , and  $6^+$  members of the ground-state rotational band were included in the coupled equations. The optical parameters used in the CC calculation were adjusted so the CC elastic scattering gave the best fit to the experimental elastic data, whereas the DWBA optical parameters were adjusted to yield the same elastic scattering as the CC result (see fig. 3). The CC calculation is thus being used as a standard against which the DWBA calculation may be compared. The optical

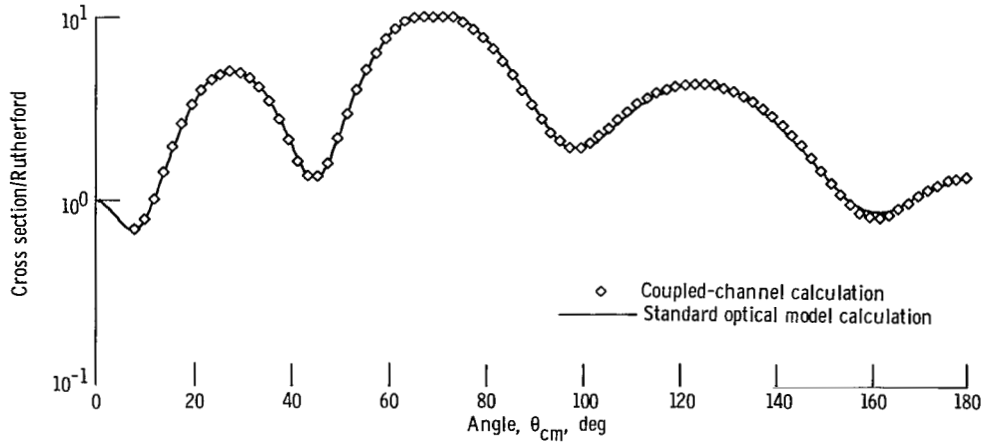


Figure 3. - Comparison of elastic scattering of 24.5-MeV protons from neon-20 predicted by coupled-channel calculation and standard optical model calculation with DWBA parameters described in the text.

TABLE III - COMPARISON OF CC AND DWBA OPTICAL  
MODEL PARAMETERS

	$V_O$ , MeV	$W_S$ , MeV	$V_{LS}$ , MeV	$r_O$ , fm	$r_S$ , fm	$r_{LS}$ , fm	$a_O$ , fm	$a_S$ , fm	$a_{LS}$ , fm
Neon-20:									
CC	55.4	7.05	3.58	1.05	1.265	0.96	0.73	0.61	0.33
DWBA	54.5	8.12	3.58	1.073	1.251	.96	.713	.61	.33
Magnesium-24:									
CC	49.1	6.56	5.29	1.174	1.19	1.06	0.736	0.562	0.546
DWBA	46.1	8.30	5.29	1.241	1.163	1.06	.665	.552	.546

parameters are listed in table III; the main difference, as one would expect, is in the imaginary surface derivative potential ( $W_S$ ), which has changed by 13 percent in going to the DWBA limit.

A comparison between CC and DWBA calculations in the largest model space (fig. 4) shows that the cross section for excitation of the  $2^+$  level is hardly changed in the DWBA limit. This is to be expected since the  $2^+$  level is predominantly coupled to the ground state. If one compares cross sections the  $4^+$  levels, however, the CC result is enhanced by a factor of about 1.7, and the angular distribution is somewhat different, particularly at larger angles. These changes are due to the double excitation through the  $2^+$  levels that cannot be accounted for in a DWBA calculation. Since the  $6^+$  level is fed by both the  $2^+$  and the  $4^+$  levels, its cross section shows an even larger deviation between DWBA and CC predictions. The discrepancy in magnitude between theory and

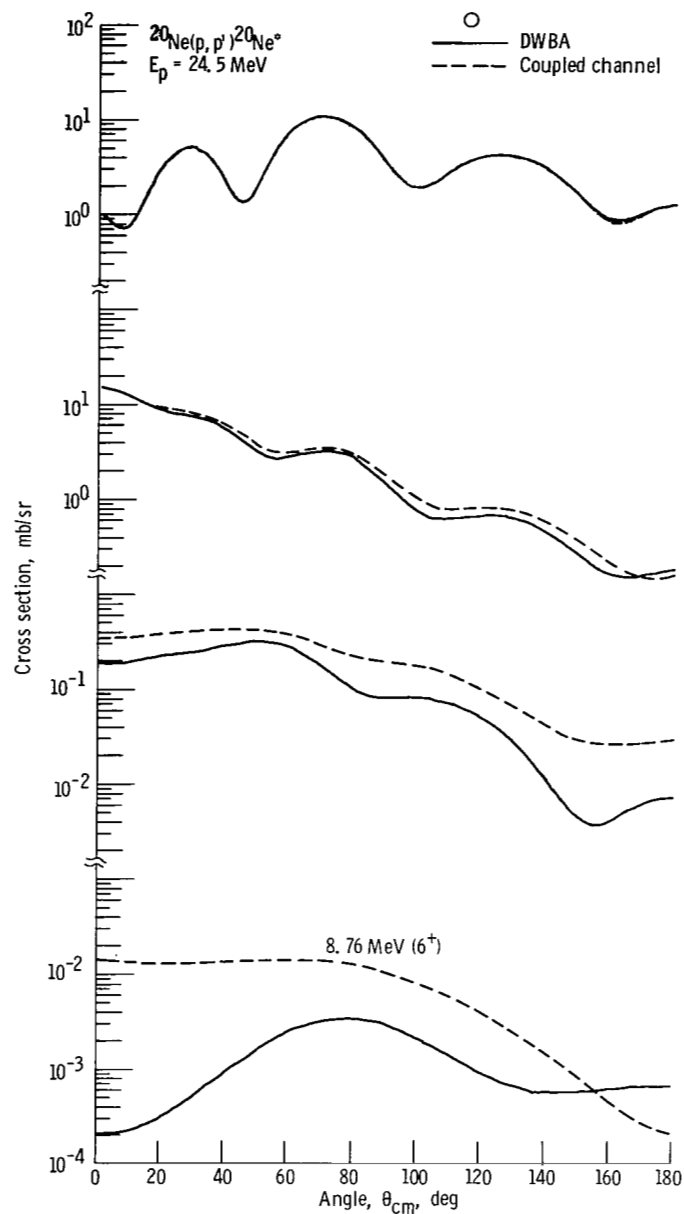


Figure 4. - Comparison of DWBA and coupled-channel predicted cross sections for scattering of 24.5-MeV protons from neon-20.

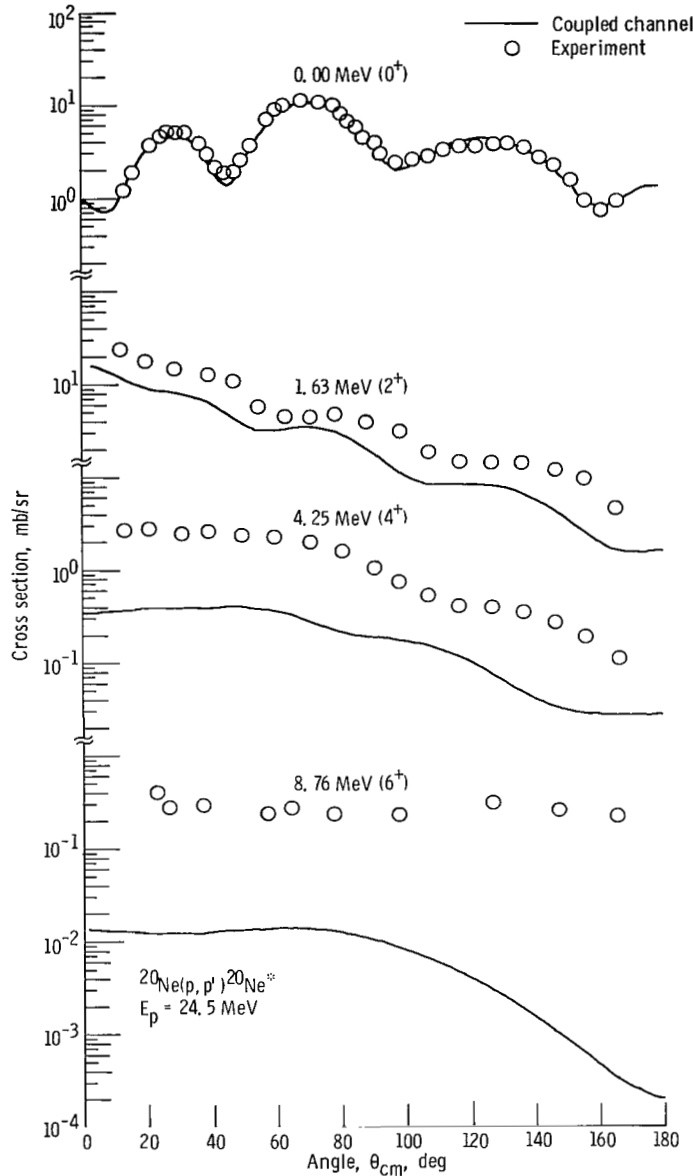


Figure 5. - Coupled channel results compared with experiment for scattering of 24.5-MeV protons from neon-20.

experiment (fig. 5) is not surprising since a bare nucleon-nucleon force is used in the scattering problem.

We have also studied how the cross sections are affected by truncation of the nuclear model space. Coupled channel and DWBA calculations were carried out with model spaces containing six, 10, and 15 basis functions, as described in table I (see also fig. 6). For the sake of simplicity these calculations were made with the same set of optical parameters which appear in table III. As one can see from figure 7, the major en-

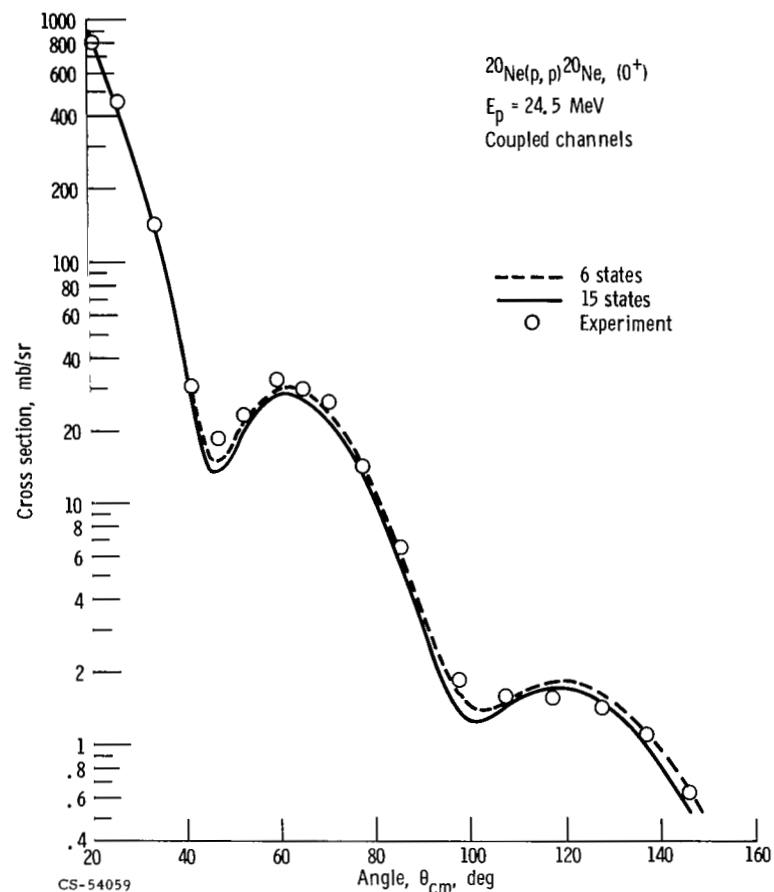


Figure 6. - Coupled-channel prediction of elastic scattering of 24.5-MeV protons from neon-20 compared with experiment. The nuclear model spaces used in the calculation contain six states and 15 states as indicated.

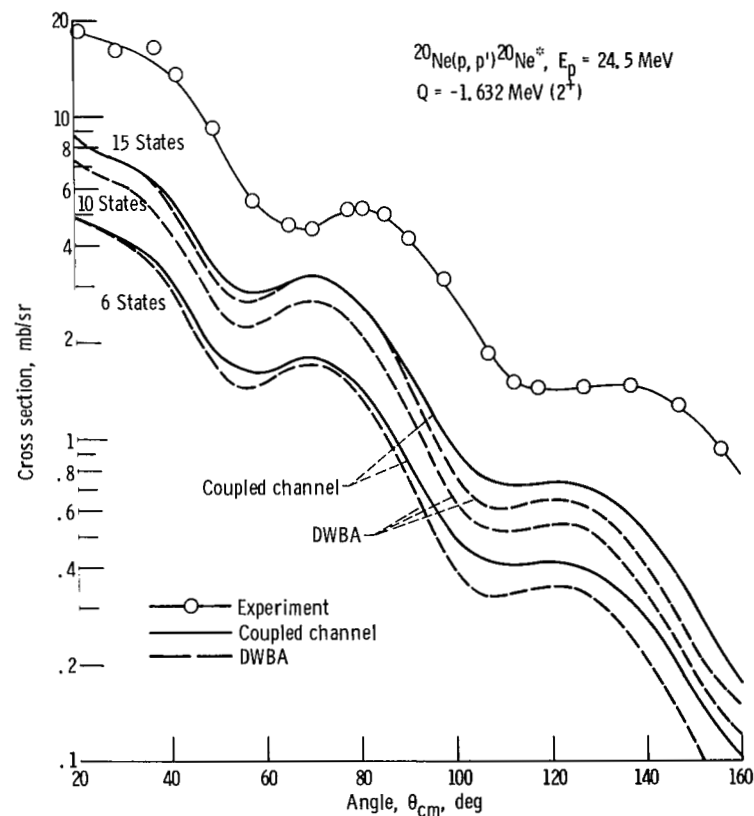


Figure 7. - Comparison of coupled-channel and DWBA predictions with experiment for excitation of the  $2^+$  ( $Q = -1.63 \text{ MeV}$ ) state in neon-20 by 24.5-MeV protons. The effect of varying the size of the model space is also indicated.

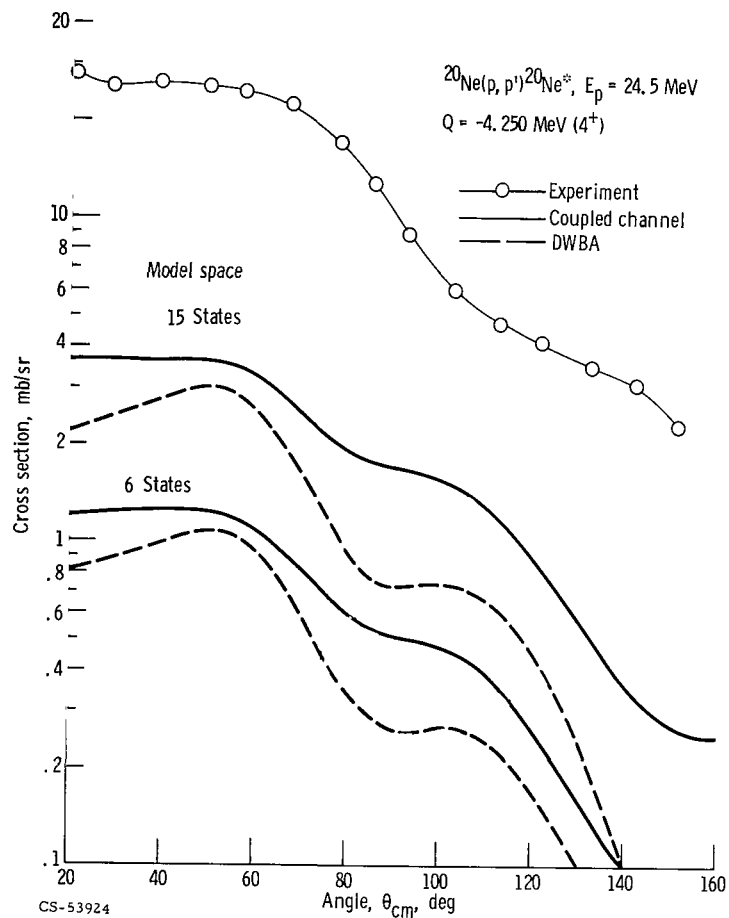


Figure 8. - Comparison of coupled-channel and DWBA predictions with experiment for excitation of  $4^+$  ( $Q = -4.25$  MeV) state in neon-20 by 24.5-MeV protons. The effect of varying the size of the model space is also indicated.

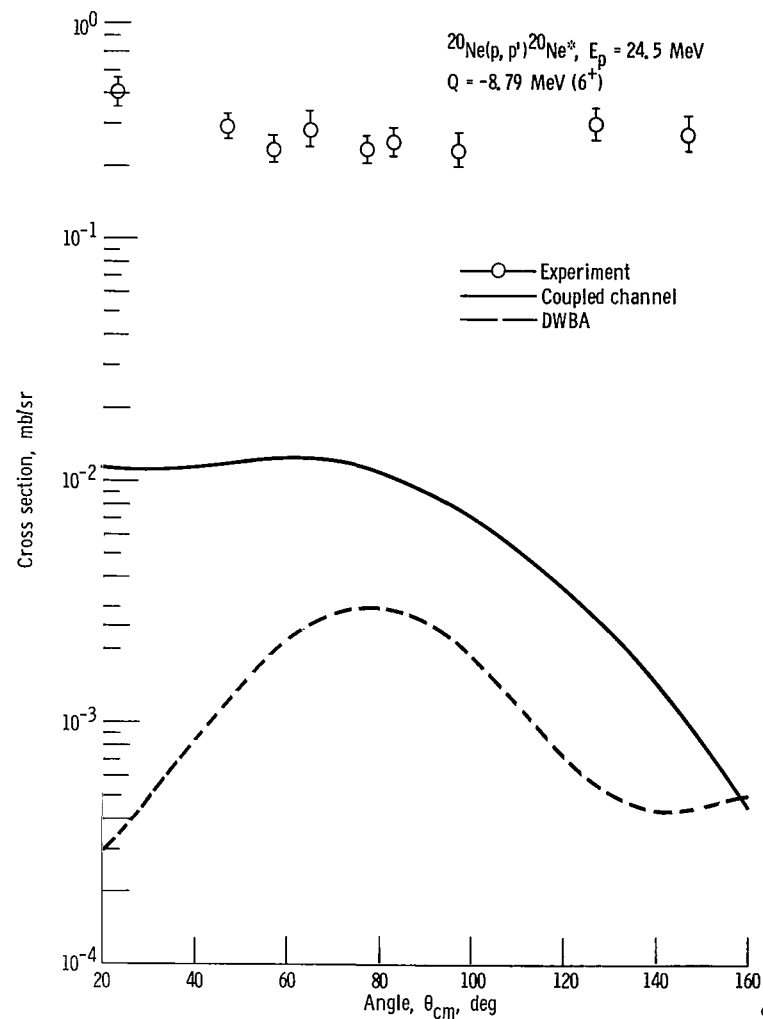


Figure 9. - Comparison of coupled-channel and DWBA predictions with experiment for excitation of  $6^+$  ( $Q = -8.79$  MeV) state in neon-20 by 24.5-MeV protons. The 15 state model space is used.

hancement of the  $2^+$  level cross section comes from the inclusion of the  $2p - 1f$  shell. No such saturation seems to be in sight for the  $4^+$  level (fig. 8). In fact, going from the 10-state to the 15-state basis increased the  $4^+$  cross section by almost a factor of two. (The plot of the 10-state result is not included because it would become difficult to read the graph). This is probably due to the inclusion of the  $1g_{7/2}$  and  $1g_{9/2}$  states that carry four units of orbital angular momentum. The magnitude of the cross section for the  $6^+$  level (fig. 9) is insignificant until one includes at least fifteen basis functions in the model space.

Similar calculations as described for  $^{20}\text{Ne}$  were carried out for the scattering of 17.5-MeV protons from  $^{24}\text{Mg}$ . The  $0^+$ ,  $2^+$ , and  $4^+$  members of the ground-state rotational band were included in the coupled equations. As before, the optical parameters used in the CC calculation were adjusted to yield a best fit to the available experimental elastic data (ref. 6), as shown in figure 10. The DWBA parameters were again chosen

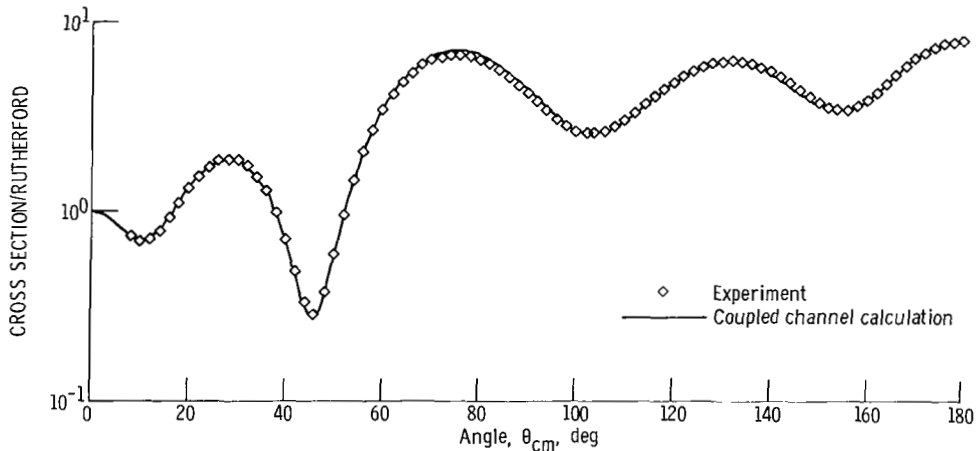


Figure 10. - Comparison of elastic scattering predicted by coupled-channel calculation and standard optical model calculation with DWBA parameters described in the text.

to yield the same elastic scattering as the CC result; see table III.

The DWBA and CC results for inelastic scattering are compared in figure 11. As in the case of  $^{20}\text{Ne}$ , the  $2^+$  cross sections are seen to be quite similar; however, the CC  $4^+$  cross section is now enhanced by almost a factor of 10 over the DWBA result. Thus, it is likely that a considerable amount of the flux to the  $4^+$  level in  $^{24}\text{Mg}$  is due to a double excitation process. The CC results are compared with experiment in figure 12. As discussed earlier, the discrepancy in magnitude between theory and experiment is not surprising. This will be discussed in greater detail in the following section.

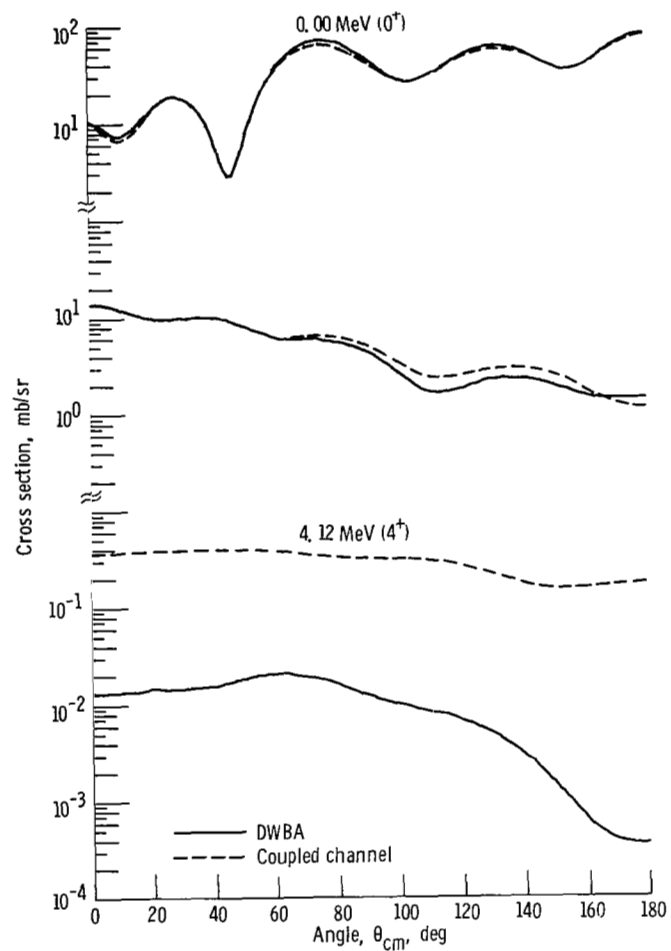


Figure 11. - Comparison of DWBA and coupled-channel predicted cross sections for the scattering of 17.5-MeV protons from magnesium-24.

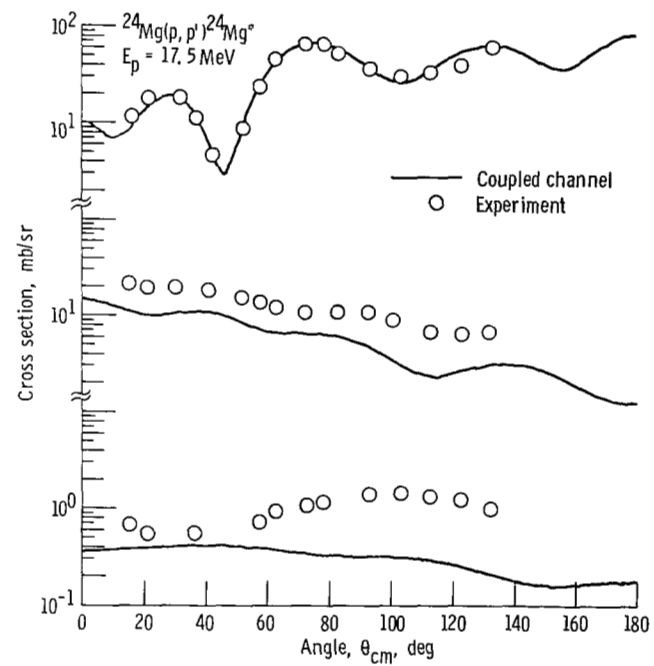


Figure 12. - Coupled-channel results compared with experiment for scattering of 17.5-MeV protons from magnesium-24.

## INSIGHTS FROM THE MACROSCOPIC MODEL

The CC-predicted cross sections for excitation of the  $2^+$  levels in both nuclei have good angular shapes when compared with experiment, and as one would expect the CC and DWBA cross sections for these levels are in close agreement. However, such is not the case for the  $4^+$  levels in these nuclei, as was noted earlier. We have found that considerable insight into this difference may be gained by examining the results of CC calculations made with the macroscopic model (ref. 6). These predictions, obtained using the collective model, appear in figures 13 and 14.

Examination of the  $^{20}\text{Ne}$  results reveals that when only quadrupole shape correlations are included, that is,  $\beta_4 = 0$ , the predicted cross sections do not compare favorably with experiment. Moreover, the quality of the shape and magnitude deteriorates as the excitation energy increases.

The next highest order in the deformation involves the hexadecapole shape parameter  $\beta_4$ . Some cross sections calculated using both quadrupole and hexadecapole terms

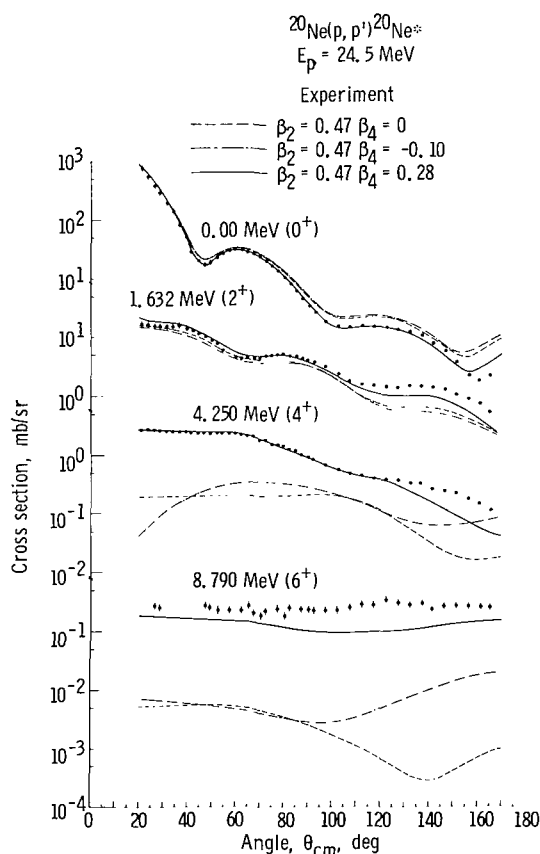


Figure 13. - Coupled-channel calculation for Neon-20 based on the macroscopic model compared with experiment. (See ref. 11.)

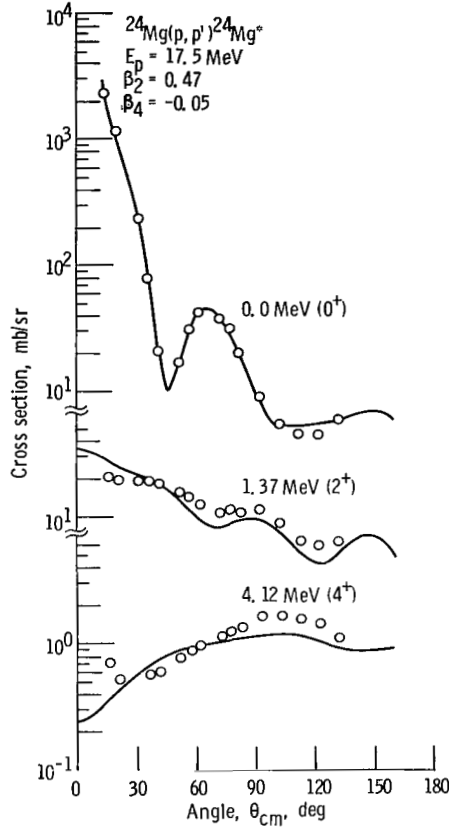


Figure 14. - Coupled-channel calculation for magnesium-24 based on macroscopic model compared with experiment. (See ref. 11.)

also appear in figure 13. The excitation of the  $2^+$  level is not affected significantly, but it is evident that the  $4^+$  cross section cannot be fit unless the deformation parameter  $\beta_4$  is given a positive value of the order of  $\beta_2^2$ . This implies that the indirect excitation ( $0^+ - 2^+ - 4^+$ ) is roughly as effective as the direct excitation ( $0^+ - 4^+$ ) in contributing to the  $4^+$  cross section. The DWBA calculation includes only the latter, and so may be expected to underestimate the CC value by about a factor of 2. This supposition, a direct inference from macroscopic model results, is borne out in our microscopic model calculations by the  $4^+$  cross sections displayed in figure 4.

Another piece of evidence may be obtained by using the fact that, judging from the macroscopic calculations, excitations of the  $6^+$  level are the most sensitive to hexadecapole deformation. A comparison of the collective model  $6^+$  cross sections shown in figure 13 to the Hartree-Fock model result shown in figure 4 suggests that the microscopic wave function does not have enough hexadecapole deformation and instead corresponds roughly to  $\beta_4 = 0$ . This in turn suggests that improvement in the microscopic wave

function could be obtained if a means were found to enhance the hexadecapole deformation.

A somewhat different situation prevails in the case of  $^{24}\text{Mg}$ . Here, the best macroscopic model fits to the data (fig. 14) are achieved for deformation parameter values such that  $|\beta_4| \ll \beta_2^2$ . Consequently one would expect the DWBA calculation of the  $4^+$  cross section, which treats only the direct excitation, to considerably underestimate the CC result. This indeed occurs, as may be seen in figure 11. Once again the HF wave function has demonstrated characteristics known to be necessary from the macroscopic studies.

We have seen that calculations of scattering cross sections performed using projected HF nuclear wave functions exhibit the same general behavior as calculations using the macroscopic model. This indicates that the moments, or shape, of the nucleus must be quite well described by the HF model. One last confirmation of this is provided by table IV, in which the nuclear moments in the intrinsic state are listed; the smallness of the  $^{24}\text{Mg}$  hexadecapole moment is striking.

TABLE IV. - MASS QUADRUPOLE

$(Q_2)$  AND HEXADECAPOLE

$(Q_4)$  MOMENTS

	$Q_2, \text{ fm}^2$	$Q_4, \text{ fm}^4$
$^{20}\text{Ne}$	83.5	304.9
$^{24}\text{Mg}$	114.5	128.6

## CONCLUSIONS

The primary object of this investigation has been to make a detailed comparison of DWBA and CC predicted cross sections and to examine, explicitly, how scattering calculations are affected by truncating the bound-state model space. The reliability of such a study ultimately depends on comparison with experiment. It is at this point that the decision must be made whether one is testing the nuclear model, the scattering mechanism, or the two-body force. In contrast to particle-transfer reactions, the mechanism for inelastic scattering of nucleons is thought to be well understood; furthermore, the Glendenning-Veneroni two-body interaction has been tested in earlier studies (ref. 14) and has yielded accurate angular distributions (although it should be mentioned

that Glendenning and Veneroni found it necessary to multiply their cross sections by factors from three to eight in order to fit the data). Thus, it was our original intention to use inelastic proton scattering as a means of testing the reliability of the best available  $^{20}\text{Ne}$  and  $^{24}\text{Mg}$  nuclear wave functions and to determine at the same time those situations in which the DWBA may be used instead of the considerably more involved CC.

The DWBA appears to be adequate for excitation of the  $2^+$  level in both  $^{20}\text{Ne}$  and  $^{24}\text{Mg}$ , but cross sections for the higher lying states are altered significantly by the CC calculation. In particular, the DWBA and CC predictions for the  $4^+$  cross section in  $^{24}\text{Mg}$  are very different, which can be understood in terms of the deformation parameters used in the macroscopic model.

A very similar difference in cross section for the  $4^+$  level in  $^{24}\text{Mg}$  was also obtained using the projected Hartree-Fock nuclear wave function, which provides gratifying evidence of the reliability of this microscopic nuclear model. After all, analysis of nuclear reactions by means of a macroscopic model essentially yields information about gross features of the nucleus, namely, its quadrupole and hexadecapole moments, as measured by the deformation parameters  $\beta_2$  and  $\beta_4$ . It now seems clear that these same general features can also be reproduced by the much more complicated many-nucleon wave function, which is determined solely from general symmetry constraints and the requirement of energy minimization.

There remain some areas of uncertainty, however. Including the active core (which was left out of Glendenning and Veneroni's calculation), enlarging the model space, and using the coupled channel method have all helped to bring the cross sections closer to agreement with experiment - but not enough. It seems unlikely that further enlargement of the bound-state model space will solve the problem. One is therefore led, somewhat reluctantly, to question the validity of the two-body force being used, and perhaps even the inelastic scattering mechanism. It is well known that the two-body force is stronger within nuclear matter than it is in vacuum, and it would not be unreasonable to expect this renormalized force to be responsible for the nuclear transition. It is also possible that effects of antisymmetrization between the projectile and the target nucleons, usually considered small and therefore ignored as part of the excitation mechanism, may in fact play a substantial role. Both these possibilities are currently under investigation.

Lewis Research Center,  
National Aeronautics and Space Administration,  
Cleveland, Ohio, July 15, 1971,  
129-02.

## REFERENCES

1. Braley, Richard C.; and Ford, William F.: Inelastic Scattering Calculations with Projected Hartree-Fock Wave Functions. *Phys. Rev.*, vol. 182, no. 4, June 20, 1969, pp. 1174-1185.
2. Glendenning, Norman K.: Coupled Channel Treatment of Inelastic Scattering Based on Microscopic Nuclear Descriptions. *Nucl. Phys.*, vol. A117, 1968, pp. 49-65.
3. Satchler, G. R.: Inelastic Scattering and the Nuclear Shell Model. *Nucl. Phys.*, vol. 77, 1966, pp. 481-512.
4. Love, W. G.; and Satchler, G. R.: Core Polarization and the Microscopic Model of Inelastic Scattering. *Nucl. Phys.*, vol. A101, 1967, pp. 424-448.
5. Buck, B.: Calculation of Elastic and Inelastic Proton Scattering with a Generalized Optical Model. *Phys. Rev.*, vol. 130, no. 2, Apr. 15, 1963, pp. 712-726.
6. de Swiniarski, R.; Glashausser, C.; Hendrie, D. L.; Sherman, J.; Bacher, A. D.; and McClatchie, E. A.: Evidence for  $1/4$  Deformation in  $^{20}\text{Ne}$  and Other s-d Shell Nuclei. *Phys. Rev. Letters*, vol. 23, no. 6, 1969, pp. 317-320.
7. Ripka, Georges: The Hartree-Fock Theory and Nuclear Deformations. *Lectures in Theoretical Physics. Vol. VIII C.* P. D. Kunz, D. A. Lind, and W. Britten, eds., Univ. of Colo. Press, 1966, pp. 237-298.
8. Ford, W. F.; and Braley, R. C.: Inelastic Transition Densities. *Nucl. Phys.*, vol. A162, 1971, pp. 513-529.
9. Ford, William F.; and Braley, Richard C.: An Efficient Method of Energy Projection. Presented at the Amer. Phys. Soc. Winter Meeting, Stanford, Calif., Dec. 28-31, 1970.
10. Amos, K. A.; Madsen, V. A.; and McCarthy, I. E.: Antisymmetrized Distorted-Wave Approximation for Nucleon-Nucleus Scattering. *Nucl. Phys.*, vol. A94, 1967, pp. 103-128.
11. Love, W. G.; and Satchler, G. R.: Exchange Effects with a Realistic Interaction for Inelastic Scattering. *Nucl. Phys.*, vol. A159, 1970, pp. 1-44.
12. Bassichis, W. H.; Pohl, B. A.; and Kerman, A. K.: The Effects of Truncation in Nuclear Hartree-Fock Calculations. *Nucl. Phys.*, vol. A112, 1968, pp. 360-371.

13. Ford, William F.; Braley, Richard C.; and Bar-Touv, J.: A Study of the Hartree-Fock Model Space for Light Deformed Nuclei. NASA TN D-6187, 1971.
14. Glendenning, Norman K.; and Veneroni, Marcel: Inelastic Scattering Based on a Microscopic Description of Nuclei. Phys. Rev., vol. 144, no. 3, Apr. 22, 1966, pp. 839-853.

OFFICIAL BUSINESS  
PENALTY FOR PRIVATE USE \$300

FIRST CLASS MAIL

POSTAGE AND FEES PAID  
NATIONAL AERONAUTICS AND  
SPACE ADMINISTRATION



010 001 C1 U 24 711001 S00903DS  
DEPT OF THE AIR FORCE  
AF SYSTEMS COMMAND  
AF WEAPONS LAB (WLOL)  
ATTN: E LOU BOWMAN, CHIEF TECH LIBRARY  
KIRTLAND AFB NM 87117

POSTMASTER: If Undeliverable (Section 158  
Postal Manual) Do Not Return

*"The aeronautical and space activities of the United States shall be conducted so as to contribute . . . to the expansion of human knowledge of phenomena in the atmosphere and space. The Administration shall provide for the widest practicable and appropriate dissemination of information concerning its activities and the results thereof."*

— NATIONAL AERONAUTICS AND SPACE ACT OF 1958

## NASA SCIENTIFIC AND TECHNICAL PUBLICATIONS

**TECHNICAL REPORTS:** Scientific and technical information considered important, complete, and a lasting contribution to existing knowledge.

**TECHNICAL NOTES:** Information less broad in scope but nevertheless of importance as a contribution to existing knowledge.

**TECHNICAL MEMORANDUMS:**  
Information receiving limited distribution because of preliminary data, security classification, or other reasons.

**CONTRACTOR REPORTS:** Scientific and technical information generated under a NASA contract or grant and considered an important contribution to existing knowledge.

**TECHNICAL TRANSLATIONS:** Information published in a foreign language considered to merit NASA distribution in English.

**SPECIAL PUBLICATIONS:** Information derived from or of value to NASA activities. Publications include conference proceedings, monographs, data compilations, handbooks, sourcebooks, and special bibliographies.

**TECHNOLOGY UTILIZATION PUBLICATIONS:** Information on technology used by NASA that may be of particular interest in commercial and other non-aerospace applications. Publications include Tech Briefs, Technology Utilization Reports and Technology Surveys.

*Details on the availability of these publications may be obtained from:*

**SCIENTIFIC AND TECHNICAL INFORMATION OFFICE**

**NATIONAL AERONAUTICS AND SPACE ADMINISTRATION**

**Washington, D.C. 20546**